Spectrochimica Acta Part A: Molecular and Biomolecular Spectroscopy 293 (2023) 122450

Contents lists available at ScienceDirect

Spectrochimica Acta Part A: Molecular and Biomolecular Spectroscopy

journal homepage: www.journals.elsevier.com/spectrochimica-acta-part-a-molecular-and-biomolecular-spectroscopy

Understanding the compositional changes of organic matter in torrefied olive mill pomace compost using infrared spectroscopy and chemometrics

Marta P. Rueda [a], Francisco Comino [a], Víctor Aranda [b], María José Ayora-Cañada [a], Ana Domínguez-Vidal [a,*]

[a] Department of Physical and Analytical Chemistry, Universidad de Jaén, Campus Las Lagunillas E-23071, Jaén, Spain
[b] Department of Geology, Universidad de Jaén, Campus Las Lagunillas E-23071, Jaén, Spain

HIGHLIGHTS

- Study of industrial OMP-compost torrefaction at different maturation stages.
- Data fusion of FT-IR & FT-NIR provide insight on thermochemical structural changes.
- At 175 °C, loss of water and protein degradation. Samples still differentiated by maturation stage.
- From 225 °C, loss of CH and OH moieties. Increase of aromatization & carbonyl groups.
- Torrefaction at 275 °C helps to stabilize unmature compost improving quality.

GRAPHICAL ABSTRACT

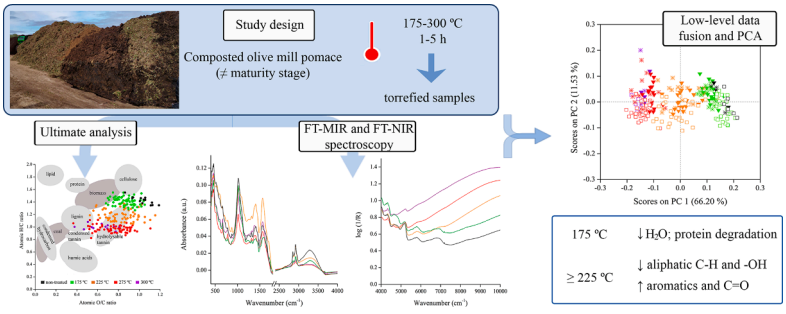

ARTICLE INFO

Keywords:
Compost
Olive mill pomace
Thermal treatment
FT-MIR
FT-NIR
Chemometrics
Organic matter

ABSTRACT

Composting olive mill pomace (OMP), the major by-product of the olive oil industry, is an attractive waste management practice in the context of sustainable food production. Thermal treatment of compost at mild temperatures (torrefaction) can aid to improve its characteristics as a soil amendment. This study aims to understand the chemical changes occurring during torrefaction of olive mill pomace-based (OMP) compost, as well as to evaluate the treatment effects on compost at different stages of maturation. Here, treatments at different temperatures (175, 225, and 275 °C) and duration (from 1 to 5 h) have been employed to obtain a sort of torrefied samples. In general, the H/C and O/C atomic ratios of compost samples decreased with torrefaction temperatures, which suggests an incipient coalification of the organic matter. Furthermore, the results showed that a combination of FT-NIR and FT-MIR spectroscopy using a low-level data fusion strategy is very sensitive to the molecular changes occurring both in the composting process and during heating. Principal Component Analysis (PCA) of the merged spectra revealed that the changes at 175 °C are mainly the loss of water (O–H contributions at 3300 and 5169 cm^{-1}) together with the degradation of proteins (observed in the decrease of amide I and II characteristic bands). Furthermore, the samples heated at this temperature can still be differentiated by their initial maturation stage. On the other hand, thermochemical changes occurring at higher temperatures are more intense and make the samples more alike, independently of the composting time. When heating above 225 °C, the loss of O–H happens together with the decrease of aliphatic moieties, reflected in the bands 2920 and 2850 cm^{-1} (FT-MIR) and 4258, 4323, 5665, and 5781 cm^{-1} (FT-MIR). This can be attributed to

* Corresponding author.
E-mail address: adovidal@ujaen.es (A. Domínguez-Vidal).

https://doi.org/10.1016/j.saa.2023.122450
Received 24 November 2022; Received in revised form 25 January 2023; Accepted 1 February 2023
Available online 4 February 2023

the thermal degradation of cellulosic materials and, additionally, to the degradation of the residual oil in the case of poorly composted samples. Heated samples are characterized by the presence of carbonyl groups (1709 cm^{-1}) and humic-like complex and polymerized aromatic structures (1579 cm^{-1}). Since the characteristics of the torrefied compost at 275 °C are very similar regardless of the initial maturation stage, torrefaction may be a very interesting way to reduce the composting time of olive mill pomace to obtain a high-quality organic amendment for soil application.

1. Introduction

Nowadays, there is an increasing concern for the achievement of a more sustainable food production chain. In this context, the valorization of by-products is one of the biggest challenges of the agro-food industry to reduce its environmental impact. In Mediterranean countries, the olive oil industry plays a key socio-economic role, accounting for over 95 % of the world's olive oil production [1]. However, this growing industry produces large quantities of by-products and wastes. Of particular concern is wet olive mill pomace (OMP), the main by-product derived from the two-phase centrifugation method for olive oil extraction. This residue is a combination of olive husk and pulp, and olive mill wastewater, with a moisture content of around 65% [2]. OMP is rich in easily degradable organic matter (OM) and has a very high organic load, with Chemical Oxygen Demand (COD) values of about 80–200 g l^{-1} [1], and significant amounts of tannins and polyphenols, which are responsible for antimicrobial activities and phytotoxicity [3]. Composting is one of the most promising options to transform these residues into a valuable soil amendment ensuring the biological degradation of the potentially harmful compounds in OMP during the process [4,5]. The use of composted OMP as an organic amendment is a valorization alternative particularly interesting since arable soils in the Mediterranean region exhibit extremely low organic C content, with values frequently below 1 % [6]. Composting OMP along with other complementary wastes, like animal manures (rich sources of nutrients as N and P), cereal straw, olives leaves, or pruning (bulking agents to increase the porosity of the matrix), has been proposed as an efficient solution for its recycling [1,7].

The composting processes must be suitably managed and the progressive changes with time of the physical–chemical characteristics of composts must be carefully controlled to give an end product with optimum quality for success after field application. In particular, compost should have stabilized OM (resistant to fast biodegradation) and the absence of phytotoxicity. The latter has been reported to be related to polyphenols and lipids content in immature OMP compost [5]. Moreover, aliphatic compounds present in the raw materials or non-evolved compost, notably increases the water repellency of the organic amendments, affecting water availability for plants and infiltration rates [3,8], leading to important environmental problems, such as increased erosion, loss of soil nutrients, and groundwater contamination [7,9]. Several factors could affect composting effectiveness, including those depending on the composting mixture's preparation (such as pH, particle size, porosity, total pile volume, initial moisture, and carbon to nitrogen ratio (C/N) and those of the process management, such as moisture content, temperature, and aeration. Infrared spectroscopy has been proposed as a useful alternative to monitor composting processes and to characterize composted materials reducing the need for expensive and time-consuming chemical analysis [10–12]. However, since the composition of the input mixture strongly affects the shape of the infrared spectra, any particular composting mixture needs dedicated studies to identify the main changes occurring during the composting process [13]. On the other hand, our previous research studies have demonstrated that the application of thermal treatments to composted materials of different origins improves their quality and safety, reducing their hydrophobicity and phytotoxicity [14,15]. Such thermal treatment at mild temperatures (175–275 °C) is, in fact, very similar to dry torrefaction, which has aroused great interest in the bioenergy sector in the last years [16,17]. Torrefaction of lignocellulosic biomass including agriculture residues has been extensively studied [18–20]. This process typically involves slow heating in the temperature range of 230–300 °C. When biomass is torrefied, moisture and carbon dioxide are removed, and the long polysaccharide chains are depolymerized, yielding a solid product of increased energy density [19]. Most studies on the torrefaction of biomass have focused on examining the mass loss, carbon content, and energy distribution with changing time and temperature of treatments for woody materials [18,21]. In addition, in some cases, the structural changes of torrefied biomass were further analyzed by spectroscopic techniques [19,22]. Nevertheless, the compositional effects induced by heating in OMP compost still need further investigation. In comparison with typical lignocellulosic biomass, OMP compost is more complex. This is first due to the variety of feedstock sources, including animal manure, in the initial composting mixture. Furthermore, the microbial degradation of biomass and the formation of humic-like substances during the composting process, make compost different from raw biomass usually employed in torrefaction studies [19,20,22]. Thus, a deep study of the OMP compost torrefaction process to understand the changes in organic matter is of interest with a view to employing it as a soil amendment. To do this, Fourier transform infrared spectroscopy, both in the middle and near-infrared region (FT-MIR and FT-NIR) will be employed to assess the changes induced by torrefaction treatments at different temperatures and with different duration. A data fusion strategy [23] will be used to combine the outputs of both IR spectral regions to exploit the synergetic and complementary information provided. The fused IR spectra will be analyzed using Principal Component Analysis (PCA) [24]. This procedure extracts the information from the original data matrix by reducing the dimensionality to a small number of principal components (PCs). PCA reveals those underlying features responsible for similarities and differences between the materials under study. The loadings vectors, corresponding to the PCs, provide information on the contribution of the spectral regions to the differentiation between samples observed in the scores plot. Here the loadings are combinations of the two regions (middle and near infrared) and can potentially result in a more comprehensive characterization of torrefied compost and the changes happening at different temperatures.

Furthermore, in this work, we will also evaluate the effects of torrefaction on OMP compost at different stages of the composting process, that is, at different maturation stages. This can be relevant to consider this treatment as an alternative way to reduce the composting time, providing a high-quality amendment for soil application in a shorter time.

2. Material and methods

2.1. Sample collection and description

Composted olive mill pomace (COMP) samples were provided by INGNIA S.L. This composting plant, located in Almedinilla (Córdoba, Spain), uses four raw materials mixed according to the following proportions: 68 % olive mill pomace (OMP), 24 % goat manure mixed with straw (GM), 6 % olive tree pruning (OTP), and 2 % chicken manure mixed with sawdust (CM). Windrow composting is approached in 4 m high and 8 m diameter piles turned regularly once a fortnight to avoid any anaerobic processes. Ten samples of compost were collected from the piles during the composting process comprising different stages of

maturity (see Table 1). Evolved compost was sampled in the final stages of the composting process (around one year) whereas non-evolved compost corresponds to material in the initial stages of the process (less than 10 weeks). Each sample involved five sub-samples collected in five different pile positions to assure representativeness. Furthermore, three samples of completed compost were considered. This term refers to materials that have been composted for >75 weeks and commercialized as finished products. All the samples were desiccated at 65 °C, then ground and sieved to 200 μm.

2.2. Torrefaction treatment

The compost samples were subjected to different dry torrefaction treatments in terms of temperature and time in a furnace oven (Carbolite Gero). To do this, about 20 g of each sample were placed in covered porcelain containers and heated up to 175, 225, and 275 °C at a 50 °C/min ramp rate and maintained at the final temperature for 1, 2, 3, 4, and 5 h. In addition, samples were heated at 300 °C for 5 h. In this way, 208 torrefied samples were obtained.

2.3. Physical-chemical characterization

The moisture content was determined by differential weighing after 24 h at 105 °C. Electrical conductivity at 25 °C (EC_{25}) and pH were measured in 1:10 (w/v) water-soluble extracts with a CRISON conductivity meter and a HANNA pH-meter respectively. Ultimate analysis in terms of percentages of carbon, hydrogen, and nitrogen in the elemental form [21] was determined using a LECO TruSpec CHN 620-100-400 analyzer. Oxygen content was estimated by difference (sulfur content was negligible in all the cases). For torrefied samples, % of mass loss and indices of decarbonization (DC), dehydrogenation (DH), deoxygenation (DO), and denitrogenation (DN) were calculated according to Chen *et al.* [25].

2.4. Infrared spectroscopy

Mid-IR spectra were recorded using a Vertex 70 FTIR Spectrometer (Bruker Corporation, Germany) equipped with an attenuated total reflection (ATR) accessory with a three-reflection diamond crystal (Platinum ATR, Bruker). Fine grinding in an agate mortar was achieved before placing the samples directly on the ATR crystal. Controlled pressure was applied to ensure good contact between the sample and the ATR element. The FT-MIR spectra ranged from 400 to 4000 cm^{-1} with a resolution of 4 cm^{-1} and 128 accumulations. Three replicates were made per sample. The spectrum of the clean ATR crystal was used as background.

Fourier transform NIR spectra were registered with an Antaris FT-NIR system (Thermo Nicolet Corp.) equipped with an integrating sphere module for diffuse reflectance measurements. Samples were placed directly into a 3 cm capsule, which was rotated during the measurement. FT-NIR spectra were collected between 4000 and 10000 cm^{-1} with a resolution of 8 cm^{-1} and 64 accumulations, each spectrum averaging three replicates. The background was automatically recorded before each measurement using the internal gold reference of the sphere.

Table 1
Samples description.

Sample	Composting time (weeks)	Maturity stage
COMP1	> 75	Completed
COMP2	> 75	Completed
COMP3	> 75	Completed
COMP4	54	Evolved
COMP5	54	Evolved
COMP6	49	Evolved
COMP7	49	Evolved
COMP8	9	Non-evolved
COMP9	9	Non-evolved
COMP10	3	Non-evolved
COMP11	3	Non-evolved
COMP12	2	Non-evolved
COMP13	2	Non-evolved

2.5. Chemometrics

Principal Component Analysis (PCA) was used to investigate changes occurring when samples were subjected to different torrefaction treatments. PCA reduces the dimensionality of large datasets by calculating principal components (PCs) that are linear combinations of the original variables retaining the relevant information contained in the original data. Score plots (showing the projections of each observation over each PC axis) are useful to detect groupings and trends among the samples. Loading plots (showing the coefficients of the original variables in the linear combinations for each PC) allows for identifying those original variables that are more relevant for each PC.

In the present work, PCA was first applied to the chemical variables of the ultimate analysis after autoscaling as pretreatment. Furthermore, FTIR spectra were analyzed merging the information of both middle and near infrared regions. To do this, a low-level data fusion strategy was applied: FT-NIR and FT-MIR spectra were concatenated after normalization to avoid scale differences and then mean-centered. All these chemometric treatments were performed using Solo + MIA software version 8.9.1 (Eigenvector Research, Inc.).

3. Results and discussion

3.1. Preliminary characterization of raw materials and composted olive mill pomace samples

An initial physical–chemical characterization of the raw materials and the compost samples is shown in Table 2. Samples at the initial stages of composting are characterized, in general, by high moisture and low pH, typical of raw OMP [26]. The high EC_{25} values can be attributed to the addition of animal manure (CM and GM) to the composting mixture, which is also responsible for a slight increase in pH. Animal manure, in particular poultry manure (CM), is added with the main purpose of increasing the nitrogen content, mostly in the form of uric acid and urea [27]. OTP, employed as a bulking agent, is characterized by low moisture and high C and H contents.

As composting proceeds, a progressive decrease in both moisture content and electrical conductivity can be observed, along with increasing pH values, leading to levels in the range of 8.5–9.5, as expected for this type of material [28]. The ultimate analysis reveals also a decrease in C and H contents with composting due to the degradation of organic matter leading to a decrease in the C/N ratio. However, there are evident differences among all the parameters in samples with similar composting times, which brings to light the difficulties of controlling the composting process at an industrial scale.

3.2. IR spectra of compost samples and raw materials

Fig. 1 shows typical FT-MIR (1a) and FT-NIR (1b) spectra of the raw materials and OMP compost samples at different stages of maturation. FTIR spectra of these materials are complex because of the overlap of bands corresponding to both mineral phases and organic matter [13]. The main bands and tentative assignments based on literature [10,11,29] are discussed below.

Beginning with the middle IR region of the spectra, the broad band centered at 3300 cm^{-1} can be attributed to the O–H stretching of hydrogen-bonded hydroxyl groups of carboxylic acids, alcohols, and phenols, as well as to O–H groups associated with cellulose, hemicellulose, lignin, and other polysaccharides. Contributions from the stretching of the N–H bonds are also found in this region. The sharp absorption bands at 2920 and 2850 cm^{-1} are attributed to the

Table 2
Characterization of samples. Mean ± Standard Deviation (n = 3).

Sample	Moisture (%)	pH	EC_{25} (dS m^{-1})	H (%)	C (%)	N (%)	C/N
COMP1	12.7 ± 0.4	9.5 ± 0.2	3.9 ± 0.2	4.47 ± 0.07	38.9 ± 0.5	3.3 ± 0.1	11.6 ± 0.5
COMP2	19.7 ± 0.9	9.1 ± 0.2	4.8 ± 0.2	4.2 ± 0.1	37.4 ± 0.6	3.1 ± 0.1	12.2 ± 0.3
COMP3	47.7 ± 0.5	8.8 ± 0.4	3.6 ± 0.2	4.7 ± 0.3	38.7 ± 1.8	2.1 ± 0.5	19 ± 5
COMP4	45 ± 1	9.1 ± 0.6	8.7 ± 0.1	4.18 ± 0.04	37.2 ± 0.6	2.8 ± 0.1	13.4 ± 0.3
COMP5	45.8 ± 0.4	8.5 ± 0.2	4.9 ± 0.1	4.1 ± 0.1	36.3 ± 0.5	2.2 ± 0.2	17 ± 1
COMP6	42 ± 1	9.0 ± 0.2	5.1 ± 0.2	4.32 ± 0.01	37.3 ± 0.4	2.6 ± 0.2	15 ± 1
COMP7	45.8 ± 0.4	8.6 ± 0.2	5.4 ± 0.7	4.67 ± 0.03	39.6 ± 0.4	2.6 ± 0.3	16 ± 2
COMP8	57.6 ± 0.8	5.5 ± 0.5	5.6 ± 0.1	5.56 ± 0.04	43.1 ± 0.2	1.9 ± 0.1	23.2 ± 0.1
COMP9	61.5 ± 0.9	9.1 ± 0.4	5.0 ± 0.8	4.59 ± 0.04	38.5 ± 0.1	2.7 ± 0.1	14.2 ± 0.3
COMP10	57.6 ± 0.8	9.9 ± 0.3	6.6 ± 0.2	4.65 ± 0.06	38.8 ± 0.6	2.5 ± 0.1	15.4 ± 0.1
COMP11	56 ± 1	8.9 ± 0.3	5.4 ± 0.3	4.8 ± 0.2	39 ± 2	2.7 ± 0.1	14.7 ± 0.9
COMP12	56.1 ± 0.2	6.3 ± 0.4	7.2 ± 0.8	5.05 ± 0.07	41.1 ± 0.2	2.2 ± 0.1	18.6 ± 0.6
COMP13	56.4 ± 0.8	5.9 ± 0.5	7.0 ± 0.8	5.05 ± 0.02	42 ± 1	1.9 ± 0.1	22 ± 1
CM	61.5 ± 0.5	8.2 ± 0.2	7.2 ± 0.3	4.15 ± 0.03	36.3 ± 0.3	3.3 ± 0.3	11 ± 1
GM	51.6 ± 0.3	7.5 ± 0.4	9.4 ± 0.3	4.4 ± 0.2	37 ± 2	1.9 ± 0.2	19 ± 1
OTP	34.3 ± 0.6	5.9 ± 0.3	1.3 ± 0.4	5.7 ± 0.2	46 ± 1	1.24 ± 0.01	37 ± 1
OMP	71.4 ± 0.9	5.2 ± 0.3	4.3 ± 0.9	5.21 ± 0.03	41.9 ± 0.5	1.3 ± 0.1	32 ± 3

COMP: composted olive mill pomace; CM: chicken manure; GM: goat manure; OTP: olive tree pruning; OMP: olive mill pomace; EC_{25}: electrical conductivity (25 °C); H: total hydrogen; C: total carbon; N: total nitrogen.

asymmetric and symmetric stretching of aliphatic C–H groups. In the case of raw OMP, these bands together with the ester C=O stretching band at 1740 cm^{-1} represent an important contribution of lipids. In fact, residual oil is an important fraction of OMP, typically ranging from 1.5 to 15 % depending on the olive cultivation region and the employed extraction method [30,31]. These aliphatic C–H features are also remarkable in OTP, GM, and non-evolved compost samples. In evolved ones, there is a clear reduction of these bands in agreement with the decrease of C and H contents observed in the ultimate analysis. Thus, the decrease of bands in the region around 2920 cm^{-1} has been used to indicate the decomposition of organic matter [10,13]. The most intense absorption bands in the FT-MIR spectra are located in the region 950–1200 cm^{-1} and can be mainly attributed to C–O stretching vibrations of polysaccharides. The sharpness observed in the band at 1014 cm^{-1} in OMP spectra can be related to pectin [32], a very abundant component in olive wastes [33]. A certain contribution of Si–O stretching vibrations around 1000 cm^{-1} cannot be disregarded due to the use of talc as a co-adjuvant during the extraction process [34]. This seems to be confirmed by the small and sharp characteristic bands of talc observed at 3676 and 669 cm^{-1} [35]. Other contributions of silicates are also observed at 779 cm^{-1} in the OTP spectrum, possibly due to soil particles present in this material. Both goat and poultry manures showed a characteristic sharp band at 873 cm^{-1}, which together with the broader band located at 1400 cm^{-1} can be attributed to $CaCO_3$. Indeed, animal manures have been reported to increase the pH of the soil when used as amendments due to the excess of $CaCO_3$ contained in the feed rations [36]. More evolved compost samples also show a higher intensity of such carbonates bands (873 and 1400 cm^{-1}), which could be the result of organic matter depletion during composting leading to a relative increase in $CaCO_3$ content. Furthermore, the microbially induced precipitation of $CaCO_3$ by ureolytic bacteria during composting can also be considered [37,38]. This process of the appearance of $CaCO_3$ in the form of biomineralization contributes to the inorganic carbon fixation and stabilization of compost. The 1720–1500 cm^{-1} region is rich in spectral features, reflecting the overlapping of a variety of C=O stretching bands of carbonyl moieties (carboxylic acids, carboxylates, amides, and ketones) as well as C=C and C=N stretching of aromatic compounds. Furthermore, the region between 1500 and 1200 cm^{-1} is assigned to different vibrations associated with waxes, fatty acids, and phenolic compounds overlap.

On the other hand, FT-NIR spectra of the studied materials exhibited similar profiles (Fig. 1b) with highly overlapping and broad bands typical of NIR absorptions due to overtone and combination modes. Bands at 5172, 6857, and 8292 cm^{-1} have been assigned to O–H vibrations of water, namely the combination of stretching and deformation, and first and second overtones, respectively [12]. These bands can also overlap with contributions of O–H vibrations of phenols and carbohydrates giving slightly shifted features [39]. The two sharp bands at 4258 and 4331 cm^{-1} are characteristic of the combination of stretching and deformation vibrations of $–CH_3$ and $–CH_2$. These bands, together with those at 5681 and 5793 cm^{-1} that correspond to the first overtone of the C–H stretching vibration, can be attributed to aliphatic chains of cellulosic materials. These are more remarkable in OMP and non-evolved compost spectra. In addition, the broad band located at around 4700 cm^{-1} is attributed to combination bands involving C–H, C=C, and C=O stretching vibrations of lipids, phenols, and other aromatic groups [39,40]. Finally, a characteristic sharp band around 7185 cm^{-1} observed in OMP is assigned to the second overtone of O–H stretching in talc (non-H-bonded).

3.3. Effects of torrefaction treatment on compost

The influence of the torrefaction temperature and time on the characteristics of compost was investigated by considering all the thermally-treated samples (208; at temperatures 175, 225, 275, and 300 °C) and the 13 non-treated samples (dried at 65 °C). PCA was used to explore both the chemical and the spectroscopic information on compost samples at different maturation stages.

3.3.1. Mass loss and ultimate analysis

The principal component analysis performed on ultimate analysis, including the mass loss during the thermal treatment also as a variable, revealed that two PCs accounted for 82.72 % of the total variance. As seen in the scores and loadings biplot of Fig. 2, there is a certain trend of differentiation of the samples according to their original maturation stage along the PC1 axis, with negative score values for almost all the completed and evolved samples. Non-evolved compost samples are more spread along the PC1 axis. This is mainly due to differences in C, N, and H content reflecting the heterogeneity of the samples. Completed compost had the most negative scores for this component due to higher

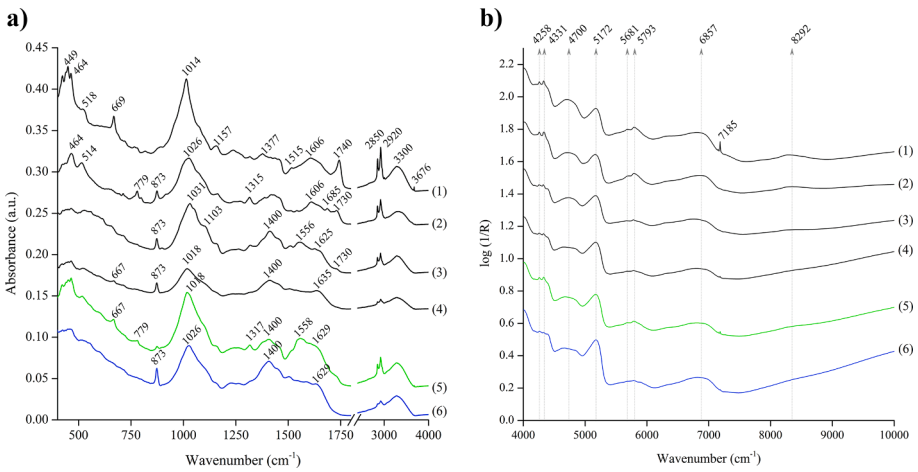

Fig. 1. Typical a) FT-MIR and b) FT-NIR spectra obtained for (1) OMP; (2) OTP; (3) GM; (4) CM; (5) non-evolved COMP and (6) evolved COMP.

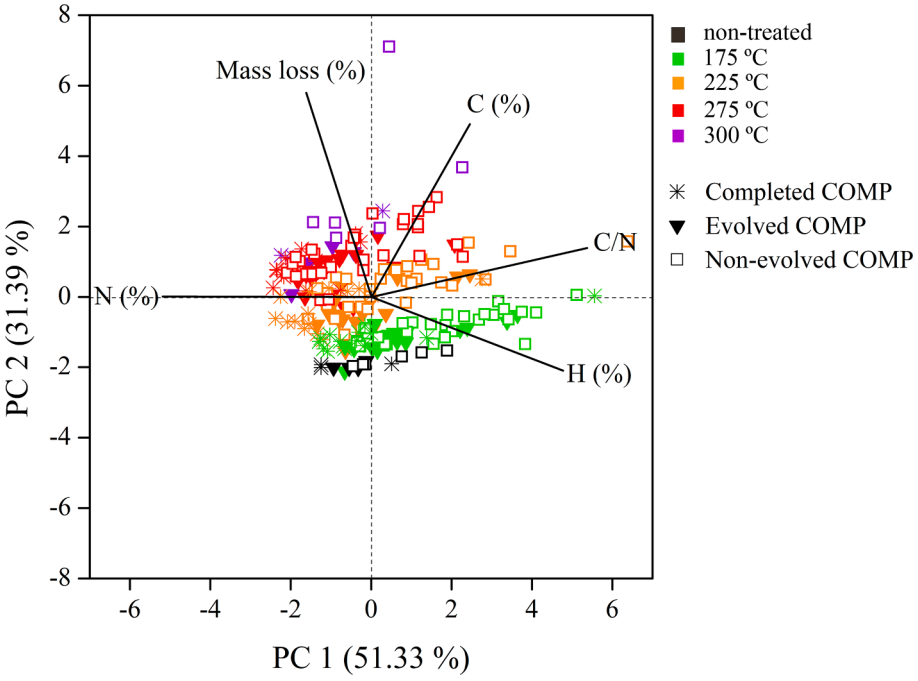

Fig. 2. PCA score-loadings biplot of the elemental determination of non- and thermally-treated COMP samples.

N contents (with negative values for the loadings of PC1), whereas non-evolved samples show higher C and H content (with positive values for the loadings of PC1), and consequently higher C/N ratio. The effect of the temperature is mainly reflected in PC2 with a clear increase in the scores values for the samples heated at higher temperatures. The percentage of mass loss is larger at increasing temperatures and particularly in less mature compost samples as can be seen from its positive value for the PC2-loading. This is due to a decrease in H content at higher temperatures whereas the C content relatively increases.

The changes happening with torrefaction can be further evaluated by calculating the indices of decarbonization (DC), dehydrogenation (DH), and deoxygenation (DO), as proposed by Chen *et al.* [25] for torrefied biomass, representing the relative loss of each element. Here, the index of denitrogenation (DN) was also included due to the relevance of this nutrient in the context of organic amendments. Fig. 3a shows the mean values for these indices at the different torrefaction temperatures considered. As can be seen, the torrefaction temperature highly influences the DH and DO, with values above 50 % of loss of these elements. On the other hand, a relatively mild effect on the C loss is shown even at 300 °C. In the case of N, it is interesting to note that its loss is higher at 175 °C than for the rest of the elements, but it remains almost constant up to 275 °C. Furthermore, it is worth mentioning that the indices of the completed materials were lower and less influenced by the temperature, indicating that more stable forms of organic matter were already present.

The removal of the different elements can be visualized in the Van Krevelen diagram by plotting atomic H/C ratios against atomic O/C ratios of both the raw and torrefied compost samples. This diagram, originally developed for the study of coals [41], takes into account that major biogeochemical classes of compounds (such as lignin compounds, lipids, carbohydrates, etc.) have their own characteristic H/C or O/C ratios and, thus, each class of compounds plots in a specific location on the diagram. As can be seen in Fig. 3b, both the H/C and O/C atomic ratios of the compost samples decreased with torrefaction temperatures, which implies a movement of the samples from the typical location of carbohydrates to the area of lignin and humic-like substances in an

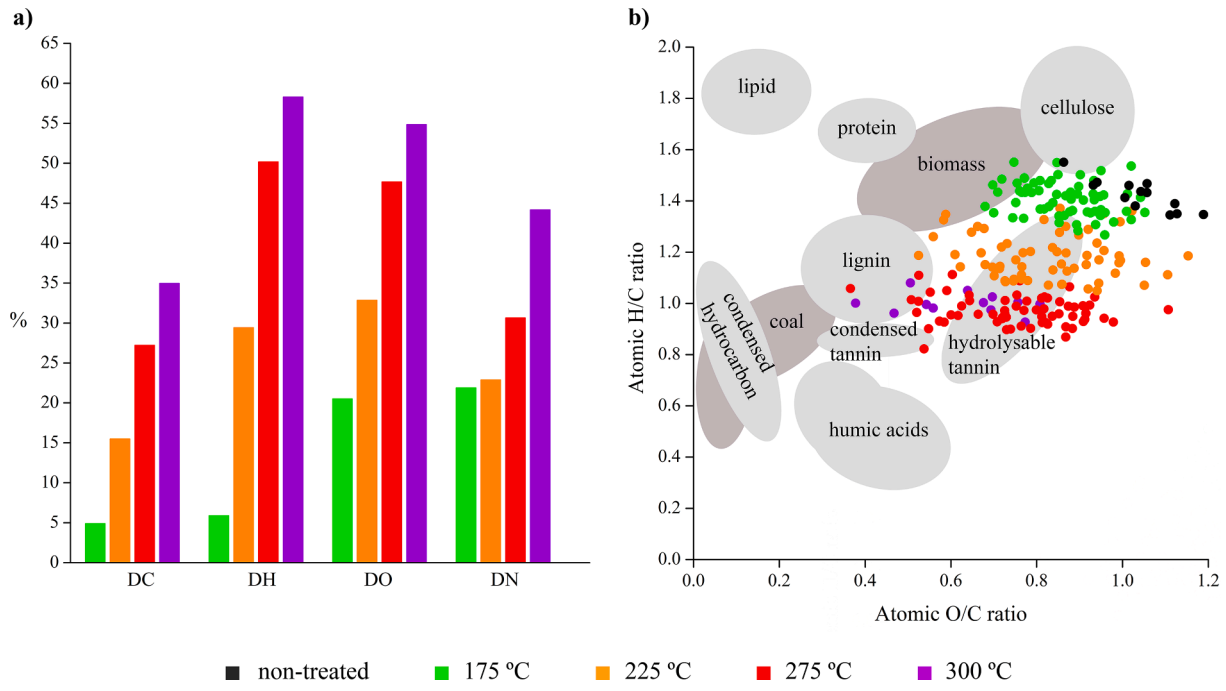

Fig. 3. a) Profiles of decarbonization (DC), dehydrogenation (DH), deoxygenation (DO), and denitrogenation (DN) of torrefied compost samples. b) Regional plots of elemental compositions from some major biomolecular components on the Van Krevelen diagram, reproduced from previous studies [43,45].

incipient coalification process [42–44]. This greater stability implies a lower rate of decomposition, and therefore, the application of these torrefied organic materials to soils could be an appropriate strategy to sequester organic carbon into the soil.

3.3.2. *Infrared spectroscopy*

The above-commented results suggest that the thermal treatments at different temperatures lead to an evident variation in the organic matter structure of the organic amendments, especially in the case of immature compost. Thus, to deepen the study of those molecular changes, FT-MIR and FT-NIR spectra were considered. Fig. 4 shows the typical spectra obtained for a non-evolved compost sample treated at different temperatures.

The most remarkable change in the FT-MIR spectra with torrefaction is the decrease in the C–H and O–H bands in the region of 2800–3600 cm^{-1}. This is consistent with the loss of aliphatic –CH_2- chains and O–H moieties suggested by the ultimate analysis and previous studies on biomass torrefaction [14]. Furthermore, a certain decrease and changes in the shape of the carbohydrate bands in the region 950–1200 cm^{-1} are observed. Other changes in the organic matter composition can be hidden by the overlap with mineral phases (mainly calcium carbonate and silicates). Concerning the FT-NIR spectra, even though the band assignment is more complex, there is a clear decrease in bands involving O–H moieties. Furthermore, it is remarkable the increase in absorption in the range above 7000 cm^{-1}. This range is influenced by particle size and especially by color changes as reported, for example, in thermally-treated wood [39]. In fact, although non-thermally treated compost samples were already dark (particularly those evolved and completed) a progressive blackening was observed with increasing temperature. This is consistent with Deng *et al.* [46], who noted a mid-brown color for biomass at low torrefaction temperatures but black for those samples heated at 300 °C.

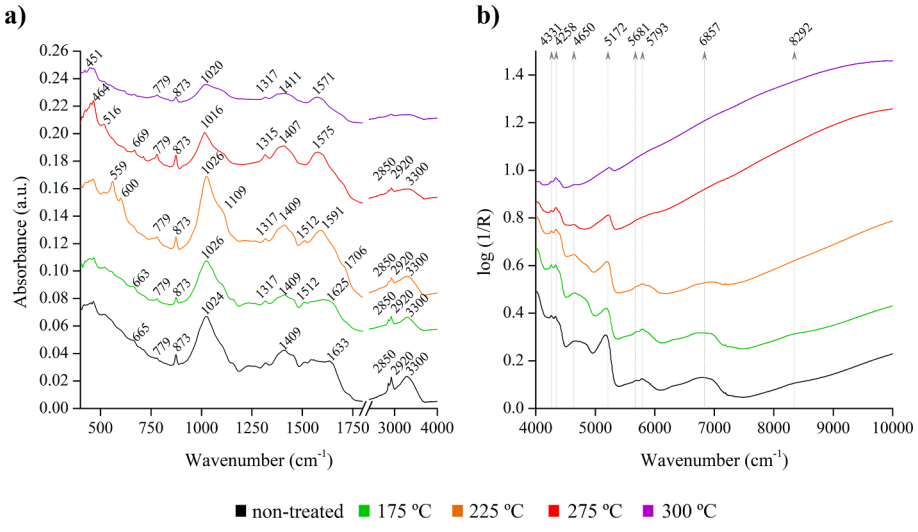

Fig. 4. Typical non-evolved COMP a) FT-MIR and b) FT-NIR spectra obtained.

A data fusion strategy was used to combine the individual information obtained from FT-MIR and FT-NIR spectra by merging them to enhance the comprehension of the data [23]. The fusion involved the concatenation of the raw data, after normalization to scale them. The results of PCA are presented in Fig. 5. The axis defined by PC1 established a clear trend in the samples according to the treatment temperature, with positive scores values for non-treated samples and those heated at 175 °C, but increasing negative values for higher temperatures. There is an overlap between the samples treated at 275 °C and 300 °C, which suggests similar changes occurring at these temperatures. The large variance collected by this component (66.20 %) indicates that the structural changes induced by temperature are the most important contribution to the differences in the infrared spectra of the compost samples.

For a better understanding of the chemical changes induced by heating as well as to evaluate how the initial stage of maturation of the compost affects its behavior, data analysis was performed separately for each temperature. Fig. 6 shows the most remarkable results of PCA of the fused infrared spectra of samples heated at each temperature (175, 225, and 275 °C) during a variable time (1 to 5 h). As can be seen in the scores plots (Fig. 6a), the effect of heating is observed along the axis defined by PC1 for 275 and 225 °C, whereas in the case of 175 °C, it is reflected by PC2. At this temperature, the main source of variance (43.78 % for PC1) is mostly related to the initial maturation stage of the composted materials. Regarding the effect of torrefaction, the percentage of variance in the spectral data induced by heating clearly increases with the temperature with values of 18.24, 53.69 and 66.68 %, for 175 , 225, and 275 °C, respectively, also reflecting the influence of the heating time. At 275 °C, there is a clear distinction between the non-treated samples and all the treated ones, which means that most of the changes occur during the first hour of the treatment. However, for lower temperatures, this distinction is not so clear. In the case of 225 °C, samples heated for 1 h are located between the non-treated and the rest, which seems to indicate that changes are still occurring after this time. Finally, with the treatment at 175 °C, the samples are spread over the PC2 axis, due to more gradual changes.

The inspection of the loadings of those PCs reflecting the changes induced by heating (as described before, Fig. 6b) provides information on the spectral changes happening at each temperature. In this way, we can access the main chemical changes gradually occurring when the temperature is increased. Considering that non-treated samples present positive scores values (for all the studied temperatures) and heated samples show lower scores values moving to negative ones for these PCs, the positive bands in the loadings represent those spectral features that are decreasing with heating. The loading vector at 175 °C shows spectral features very different from those at 225 and 275 °C. When the temperature increases above 225 °C, the marked slope of the loading vector in the NIR region reflects the already mentioned increase of absorption in the high wavenumber region (from 7000 cm^{-1}) and the loss of the main spectral features. In the middle IR region, the loss of aliphatic moieties (2920 and 2850 cm^{-1}) is clearly observed for both temperatures. In fact, this reduction of C–H groups is also reflected in the decrease in the bands at 4258, 4323, 5665, and 5781 cm^{-1} in the near IR region when applying 275 °C. In addition, the observed decrease of O–H stretching at 3280 cm^{-1} and the loss of C-O at 1028 cm^{-1} can be attributed to the thermal degradation of cellulosic materials. Similar findings have been reported for the torrefaction of biomass [22], including olive mill pomace [20]. This is also observed in the NIR region at 6283 and 6660 cm^{-1} (attributed to the first overtone of hydrogen-bonded O–H stretching) [39,47]. Furthermore, the difference in the ratio of the bands related to C–H and O–H bonds in the MIR region of the loading vector suggests that the loss of O–H moieties through dehydroxylation and dehydration reactions seems to be prominent at 225 °C, whereas the degradation of aliphatic chains is more relevant at 275 °C. Other differences in the loadings obtained for both temperatures are also related to cellulosic materials. These are the presence of a band at 993 cm^{-1} (at 225 °C) that can be attributed to a higher degradation of hemicellulose at this temperature [22], together with the difference in the position of a NIR band (4810 *vs* 4750 cm^{-1}) assigned to the combination of O–H stretching, O–H deformation, and C–H deformation [39].

The changes due to heating at 175 °C are mainly reflected in the features of the loading vector of PC2. The decrease of adsorbed water is observed in both middle (O–H stretching, broad contribution around 3300 cm^{-1}) and near IR spectra (combination of stretching and deformation of O–H bonds at 5169 cm^{-1}). Furthermore, the decreasing bands at 1645 and 1540 cm^{-1} can be assigned to C = O stretching vibrations of the peptide bonds (amide I), and C-N stretching vibrations in

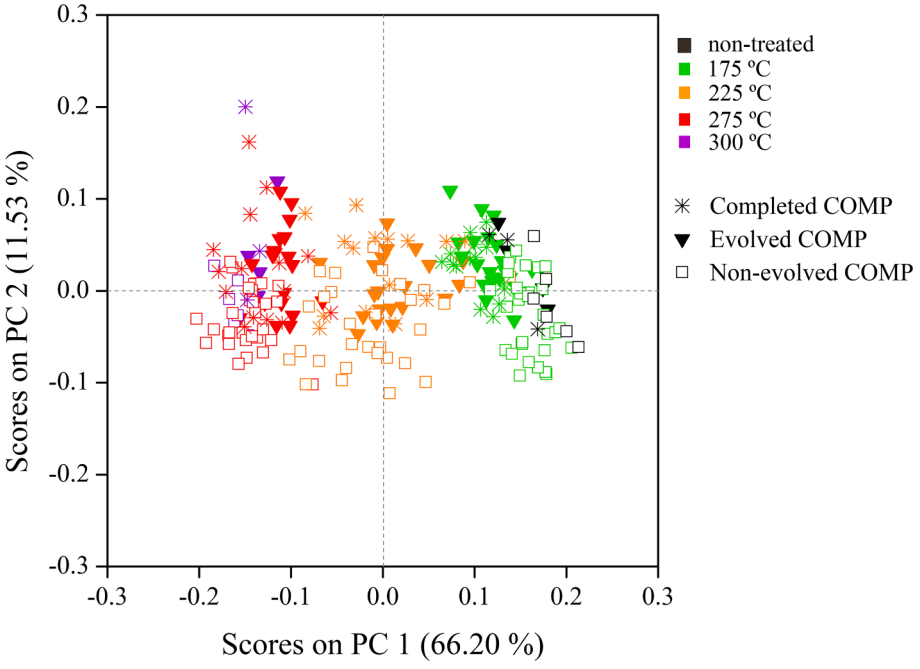

Fig. 5. PCA score plot of infrared spectra of both non- and thermally-treated COMP samples.

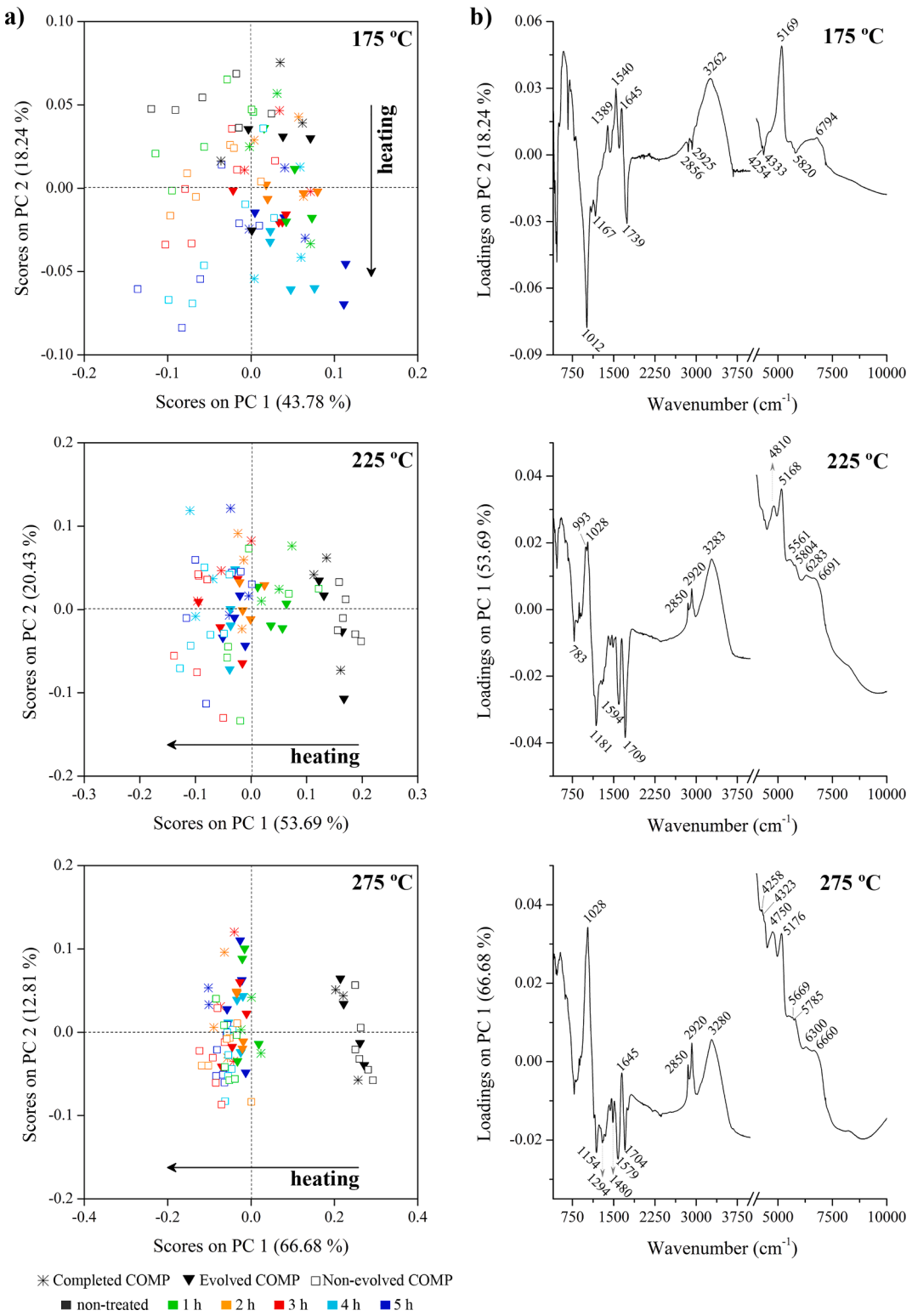

Fig. 6. Remarkable PCA results for the analysis of data fused infrared spectra at 175, 225, and 275 °C. a) Scores plots. Samples are labeled according to the time of heating at each temperature and maturation. b) Loadings vectors of PCs carrying the information related to heating.

combination with N–H bending (amide II), whereas N–H stretching contribution overlaps with O–H absorption. Thus, it can be assumed that the thermal degradation of proteins is the main process that happens at low temperatures when heating the compost samples. This effect has not been described for biomass torrefaction and it can be explained by the higher protein content in compost. Together with cellular protein from microbes, the presence of animal manure must be considered a considerable source of protein, ranging from 12 to 48 % (w/w), depending on the origin and the growth period [48].

On the other hand, negative bands in the loadings are characteristic of the heated samples. When heating at 225 and 275 °C, the negative values only appear in the region from 1100 to 1720 cm^{-1}, with slight differences in band position and relative band intensities. First, the band around 1709 cm^{-1} is characteristic of the C=O stretching of ketones or

carboxylic [49]. The presence of carboxyl groups is related to the cation exchange capacity of organic matter. This is important in soil amendments because it increases the ability of soil to retain essential nutrients. Moreover, the band around 1579 cm^{-1} can be attributed to aromatic compounds and N-heterocycles due to C=C, and C=N stretching modes [10,50]. In addition, the asymmetric COO^- stretching of carboxylates can also contribute to this band [51]. The increase in infrared bands related to aromatization agrees with the chemical changes observed during the biomass torrefaction [19,22,52] and, in general, during the composting process, with the formation of aromatic structures, such as humic-like and fulvic-like substances, and the decomposition of readily degradable organic compounds. Finally, the bands appearing at 1181 cm^{-1} (225 °C) and 1154 cm^{-1} (275 °C) are typically assigned to glycosidic linkages [32]. As the bands are negative in the loading vectors, they reflect features that are produced or conserved in heated samples. This seems to be in contradiction with the fact that depolymerization processes of cellulose and hemicellulose, involving the scission of the glycosidic linkage, are strongly favored at these temperatures [53,54]. However, taking into account the complexity of OMP compost, the presence of proteins together with polysaccharides can lead to different reactions upon heating. For example, the Maillard reaction under water-free conditions has been reported to produce melanoidins (dark brown to black colored condensation products of sugars and amino acids) showing a significant amount of di- and oligomer carbohydrates incorporated into the melanoidin skeleton with intact glycosidic bonds [55]. This would also explain the fact that the denitrogenation index (DN) did not increase at higher temperatures, which suggests the transformation of labile forms of this element into more stable structures like N-heterocycles. On the other hand, in-plane C–H deformation of aromatic rings from lignin as well as condensed tannins and polyphenols (probably oxidized and polymerized into complex humic-like substances [56–58]) can also contribute to the presence of bands around 1180 cm^{-1} in heated samples, reflecting the increasing aromatic character of these materials. It should be noted that polyphenols and melanoidins are chelating substances capable of facilitating the transport of essential nutrients to the plant and favoring its growth [59].

Finally, regarding the model at 175 °C, the most important negative features here are the bands at 1012 and 1739 cm^{-1} that can be attributed to pectin. In particular, the latter is characteristic of pectin with a high degree of methylation and can be assigned to the esterified galacturonic acids [32]. Pectic polysaccharides are abundant in OMP and their extracts show a higher degree of methyl-esterification, in comparison with pectins from other sources [60]. As can be seen in the scores plot at 175 °C (Fig. 6a), samples heated for a longer time show negative score values independently of their initial maturation stage; thus, all of them are characterized by the bands of pectin. These results suggest that pectin is more resistant both to microbial degradation during maturation and heating at lower temperatures than other polysaccharides. With higher temperatures, demethylation of pectin occurs and the band at 1740 cm^{-1} is not present in the loading vectors. As already mentioned, it has to be taken into account that the major variance in the model at 175 °C (PC1, 43.78 %), does not correspond to changes due to heating but to the initial maturation stage of the samples. Its loading vector (see Figure S1 in Supplementary material) reflects the degradation of residual oil present in OMP, as well as the increase in carbonate bands as already mentioned in the description of the raw spectra. Furthermore, the isolation of the changes occurring during maturation clarifies the alteration of polysaccharides during composting. For example, the decrease in the band at 1160 cm^{-1} shows the depolymerization due to the rupture of glycosidic linkages during composting. Additionally, the loading vector reflects changes in bands at 1011, 1035, and 1095 cm^{-1} that can be attributed to the loss of C–O bonds in cellulose and hemicellulose.

Interestingly, when heating at higher temperatures, samples cannot be discriminated against anymore according to their initial maturation stage. The spectral variability explained by PC2 and successive components only reflects the heterogeneity of the individual samples. Thus, when heating poorly composted samples degradation of residual oil and most labile polysaccharides takes place and the resulting torrefied materials have very similar properties to those obtained from more evolved compost.

4. Conclusions

Thermochemical conversion of composted olive mill pomace through torrefaction treatment is a way to transform incompletely composted materials into more stable forms of organic matter. Ultimate analysis and infrared spectroscopy revealed different characteristics for torrefied samples subjected to different thermal treatments in terms of temperature and duration. The fusion of the information contained in FT-NIR and FT-MIR spectra allowed for understanding the structural changes occurring in compost organic matter. Major chemical changes involved a carbonization phenomenon, with an increase in the content of aromatic structures due to dehydrogenation and deoxygenation processes above 225 °C. At 275 °C demethylation processes became more important, leading to a concentration of aromatic and recalcitrant compounds. Such an effect was accomplished with just 1 h of treatment at 275 °C, whereas at least 2–3 h were necessary when applying 225 °C. Few changes were induced at 175 °C, being the degradation of proteins the more relevant aspect. Additionally, in poorly composted samples, the degradation of the residual oil and labile polysaccharides was also achieved during torrefaction. In this way, the resulting materials when heating at 275 °C were very similar regardless of the starting maturation stage. Thus, torrefaction may turn out to be an attractive way to reduce composting time and obtain a stabilized high-quality organic amendment to be used in soil.

CRediT authorship contribution statement

Marta P. Rueda: Data curation, Formal analysis, Writing – original draft. **Francisco Comino:** . **Víctor Aranda:** Conceptualization, Writing – review & editing, Project administration, Funding acquisition. **María José Ayora-Cañada:** Conceptualization, Investigation, Writing – review & editing, Project administration, Funding acquisition, Supervision. **Ana Domínguez-Vidal:** Conceptualization, Investigation, Writing – review & editing, Supervision.

Declaration of Competing Interest

The authors declare that they have no known competing financial interests or personal relationships that could have appeared to influence the work reported in this paper.

Data availability

Data will be made available on request.

Acknowledgements

This work has been financed by the research projects PID2020-118673RB-I00 (Spanish Ministry of Science and Innovation) and UJA-1381060 (cofinanced by Programa operativo FEDER 2014-2020 and Consejería de Economía y Conocimiento, Junta de Andalucía). Technical and human support from the CICT-Universidad de Jaén is acknowledged (UJA, MINECO, Junta de Andalucía, FEDER).

Appendix A. Supplementary material

Supplementary data to this article can be found online at https://doi.org/10.1016/j.saa.2023.122450.

References

[1] A.K.M. Muktadirul Bari Chowdhury, C.S. Akratos, D. V. Vayenas, S. Pavlou, Olive mill waste composting: A review, Int. Biodeterior. Biodegrad. 85 (2013) 108–119. doi:10.1016/j.ibiod.2013.06.019.

[2] T.B. Ribeiro, A.L. Oliveira, C. Costa, J. Nunes, A.A. Vicente, M. Pintado, Total and sustainable valorisation of olive pomace using a fractionation approach, Appl. Sci. 10 (2020) 6785, https://doi.org/10.3390/app10196785.

[3] A.C. Barbera, C. Maucieri, V. Cavallaro, A. Ioppolo, G. Spagna, Effects of spreading olive mill wastewater on soil properties and crops, a review, Agric. Water Manag. 119 (2013) 43–53, https://doi.org/10.1016/j.agwat.2012.12.009.

[4] G. Gigliotti, P. Proietti, D. Said-Pullicino, L. Nasini, D. Pezzolla, L. Rosati, P. R. Porceddu, Co-composting of olive husks with high moisture contents: Organic matter dynamics and compost quality, Int. Biodeterior. Biodegrad. 67 (2012) 8–14, https://doi.org/10.1016/j.ibiod.2011.11.009.

[5] G.A. Baddi, J.A. Alburquerque, J. Gonzálvez, J. Cegarra, M. Hafidi, Chemical and spectroscopic analyses of organic matter transformations during composting of olive mill wastes, Int. Biodeterior. Biodegrad. 54 (2004) 39–44, https://doi.org/10.1016/j.ibiod.2003.12.004.

[6] J. Romanyà, P. Rovira, An appraisal of soil organic C content in Mediterranean agricultural soils, Soil Use Manag. 27 (2011) 321–332, https://doi.org/10.1111/j.1475-2743.2011.00346.x.

[7] R. Canet, F. Pomares, B. Cabot, C. Chaves, E. Ferrer, M. Ribó, M.R. Albiach, Composting olive mill pomace and other residues from rural southeastern Spain, Waste Manag. 28 (2008) 2585–2592, https://doi.org/10.1016/j.wasman.2007.11.015.

[8] S. Donn, R.E. Wheatley, B.M. McKenzie, K.W. Loades, P.D. Hallett, Improved soil fertility from compost amendment increases root growth and reinforcement of surface soil on slopes, Ecol. Eng. 71 (2014) 458–465, https://doi.org/10.1016/j.ecoleng.2014.07.066.

[9] F. Sellami, S. Hachicha, M. Chtourou, K. Medhioub, E. Ammar, Maturity assessment of composted olive mill wastes using UV spectra and humification parameters, Bioresour. Technol. 99 (2008) 6900–6907, https://doi.org/10.1016/j.biortech.2008.01.055.

[10] E. Smidt, K. Meissl, The applicability of Fourier transform infrared (FT-IR) spectroscopy in waste management, Waste Manag. 27 (2007) 268–276, https://doi.org/10.1016/j.wasman.2006.01.016.

[11] G. Ait Baddi, M. Hafidi, V. Gilard, J.-C. Revel, Characterization of humic acids produced during composting of olive mill wastes: elemental and spectroscopic analyses (FTIR and 13 C-NMR), EDP Sci. 23 (2003), https://doi.org/10.1051/agro:2003042ï.

[12] A. Vergnoux, M. Guiliano, Y. Le Dréau, J. Kister, N. Dupuy, P. Doumenq, Monitoring of the evolution of an industrial compost and prediction of some compost properties by NIR spectroscopy, Sci. Total Environ. 407 (2009) 2390–2403, https://doi.org/10.1016/j.scitotenv.2008.12.033.

[13] M. Grube, J.G. Lin, P.H. Lee, S. Kokorevicha, Evaluation of sewage sludge-based compost by FT-IR spectroscopy, Geoderma. 130 (2006) 324–333, https://doi.org/10.1016/J.GEODERMA.2005.02.005.

[14] F. Comino, V. Aranda, A. Domínguez-Vidal, M.J. Ayora-Cañada, Thermal destruction of organic waste hydrophobicity for agricultural soils application, J. Environ. Manage. 202 (2017) 94–105, https://doi.org/10.1016/j.jenvman.2017.07.024.

[15] F. Comino, V. Aranda, A. Domínguez-Vidal, M.J. Ayora-Cañada, Improvement of quality and agronomic properties of raw organic amendment mixtures by thermal treatment, J. Mater. Cycles Waste Manag. 22 (2020) 159–166, https://doi.org/10.1007/s10163-019-00923-4.

[16] W.H. Chen, S.H. Liu, T.T. Juang, C.M. Tsai, Y.Q. Zhuang, Characterization of solid and liquid products from bamboo torrefaction, Appl. Energy. 160 (2015) 829–835, https://doi.org/10.1016/j.apenergy.2015.03.022.

[17] L.J.R. Nunes, J.C.O. Matias, J.P.S. Catalão, A review on torrefied biomass pellets as a sustainable alternative to coal in power generation, Renew. Sustain. Energy Rev. 40 (2014) 153–160, https://doi.org/10.1016/j.rser.2014.07.181.

[18] A. Pimchuai, A. Dutta, P. Basu, Torrefaction of agriculture residue to enhance combustible properties, Energy and Fuels. 24 (2010) 4638–4645, https://doi.org/10.1021/ef901168f.

[19] C. Chen, R. Yang, X. Wang, B. Qu, M. Zhang, G. Ji, A. Li, Effect of in-situ torrefaction and densification on the properties of pellets from rice husk and rice straw, Chemosphere. 289 (2022), 133009, https://doi.org/10.1016/j.chemosphere.2021.133009.

[20] V. Benavente, A. Fullana, Torrefaction of olive mill waste, Biomass Bioenergy. 73 (2015) 186–194, https://doi.org/10.1016/j.biombioe.2014.12.020.

[21] P. Tanger, J.L. Field, C.E. Jahn, M.W. DeFoort, J.E. Leach, Biomass for thermochemical conversion: targets and challenges, Front. Plant Sci. 4 (2013) 218, https://doi.org/10.3389/fpls.2013.00218.

[22] W.H. Chen, K.M. Lu, C.M. Tsai, An experimental analysis on property and structure variations of agricultural wastes undergoing torrefaction, Appl. Energy. 100 (2012) 318–325, https://doi.org/10.1016/j.apenergy.2012.05.056.

[23] E. Borràs, J. Ferré, R. Boqué, M. Mestres, L. Aceña, O. Busto, Data fusion methodologies for food and beverage authentication and quality assessment - a review, Anal. Chim. Acta. 891 (2015) 1–14, https://doi.org/10.1016/j.aca.2015.04.042.

[24] I.T. Jolliffe, Principal Component Analysis, 2nd ed., Springer New York, NY, 2002. doi:10.1007/b98835.

[25] Y.C. Chen, W.H. Chen, B.J. Lin, J.S. Chang, H.C. Ong, Impact of torrefaction on the composition, structure and reactivity of a microalga residue, Appl. Energy. 181 (2016) 110–119, https://doi.org/10.1016/j.apenergy.2016.07.130.

[26] A. Roig, M.L. Cayuela, M.A. Sánchez-Monedero, An overview on olive mill wastes and their valorisation methods, Waste Manag. 26 (2006) 960–969, https://doi.org/10.1016/j.wasman.2005.07.024.

[27] K.H. Nahm, Evaluation of the nitrogen content in poultry manure, Worlds. Poult. Sci. J. 59 (2003) 77–88, https://doi.org/10.1079/WPS20030004.

[28] M.L. Cayuela, P. Millner, J. Slovin, A. Roig, Duckweed (Lemna gibba) growth inhibition bioassay for evaluating the toxicity of olive mill wastes before and during composting, Chemosphere. 68 (2007) 1985–1991, https://doi.org/10.1016/j.chemosphere.2007.02.064.

[29] M.E. Parolo, M.C. Savini, R.M. Loewy, Characterization of soil organic matter by FT-IR spectroscopy and its relationship with chlorpyrifos sorption, J. Environ. Manage. 196 (2017) 316–322, https://doi.org/10.1016/j.jenvman.2017.03.018.

[30] S.M. Niknam, M. Kashaninejad, I. Escudero, M.T. Sanz, S. Beltrán, J.M. Benito, Valorization of olive mill solid residue through ultrasound-assisted extraction and phenolics recovery by adsorption process, J. Clean. Prod. 316 (2021), 128340, https://doi.org/10.1016/j.jclepro.2021.128340.

[31] B. Muik, B. Lendl, A. Molina-Díaz, L. Pérez-Villarejo, M.J. Ayora-Cañada, Determination of oil and water content in olive pomace using near infrared and Raman spectrometry. A comparative study, in: Anal. Bioanal. Chem., Springer, 2004: pp. 35–41. doi:10.1007/s00216-004-2493-5.

[32] X. Liu, C.M.G.C. Renard, S. Bureau, C. Le Bourvellec, Revisiting the contribution of ATR-FTIR spectroscopy to characterize plant cell wall polysaccharides, Carbohydr. Polym. 262 (2021), 117935, https://doi.org/10.1016/j.carbpol.2021.117935.

[33] M.A. Coimbra, S.M. Cardoso, J.A. Lopes-Da-Silva, Olive pomace, a source for valuable Arabinan-rich pectic polysaccharides, in: Top. Curr. Chem., Springer, Berlin, Heidelberg, 2010, pp. 129–141. doi:10.1007/128_2010_60.

[34] F. Caponio, G. Squeo, G. Difonzo, A. Pasqualone, C. Summo, V.M. Paradiso, Has the use of talc an effect on yield and extra virgin olive oil quality? J. Sci. Food Agric. 96 (2016) 3292–3299, https://doi.org/10.1002/jsfa.7658.

[35] J. Madejová, W.P. Gates, S. Petit, IR Spectra of Clay Minerals, in: Dev. Clay Sci., Elsevier, 2017: pp. 107–149. doi:10.1016/B978-0-08-100355-8.00005-9.

[36] B. Eghball, Liming effects of beef cattle feedlot manure or compost, Commun. Soil Sci. Plant Anal. 30 (1999) 2563–2570, https://doi.org/10.1080/00103629909370396.

[37] D.A.C. Manning, P. Renforth, E. Lopez-Capel, S. Robertson, N. Ghazireh, Carbonate precipitation in artificial soils produced from basaltic quarry fines and composts: An opportunity for passive carbon sequestration, Int. J. Greenh. Gas Control. 17 (2013) 309–317, https://doi.org/10.1016/j.ijggc.2013.05.012.

[38] N.K. Dhami, M.S. Reddy, M.S. Mukherjee, Biomineralization of calcium carbonates and their engineered applications: a review, Front. Microbiol. 4 (2013) 314, https://doi.org/10.3389/fmicb.2013.00314.

[39] M. Schwanninger, J.C. Rodrigues, K. Fackler, A review of band assignments in near infrared spectra of wood and wood components, J. Near Infrared Spectrosc. 19 (2011) 287–309.

[40] C.N.T. Frizon, G.A. Oliveira, C.A. Perussello, P.G. Peralta-Zamora, A.M. O. Camlofski, Ü.B. Rossa, R. Hoffmann-Ribani, Determination of total phenolic compounds in yerba mate (Ilex paraguariensis) combining near infrared spectroscopy (NIR) and multivariate analysis, LWT. 60 (2015) 795–801, https://doi.org/10.1016/j.lwt.2014.10.030.

[41] D. Van Krevelen, Graphical statistical method for the study of structure and reaction processes of coal, Fuel. 29 (1950) 269–284, https://doi.org/10.20710/DOJO.81.2_162.

[42] S. Kim, R.W. Kramer, P.G. Hatcher, Graphical method for analysis of ultrahigh-resolution broadband mass spectra of natural organic matter, the Van Krevelen diagram, Anal. Chem. 75 (2003) 5336–5344, https://doi.org/10.1021/ac034415p.

[43] W.C. Hockaday, A.M. Grannas, S. Kim, P.G. Hatcher, The transformation and mobility of charcoal in a fire-impacted watershed, Geochim. Cosmochim. Acta. 71 (2007) 3432–3445, https://doi.org/10.1016/j.gca.2007.02.023.

[44] P.M. Trompowsky, V. De Melo Benites, B.E. Madari, A.S. Pimenta, W.C. Hockaday, P.G. Hatcher, Characterization of humic like substances obtained by chemical oxidation of eucalyptus charcoal, Org. Geochem. 36 (2005) 1480–1489, https://doi.org/10.1016/j.orggeochem.2005.08.001.

[45] M.J. Prins, K.J. Ptasinski, F.J.J.G. Janssen, From coal to biomass gasification: comparison of thermodynamic efficiency, Energy. 32 (2007) 1248–1259, https://doi.org/10.1016/j.energy.2006.07.017.

[46] J. Deng, G.J. Wang, J.H. Kuang, Y.L. Zhang, Y.H. Luo, Pretreatment of agricultural residues for co-gasification via torrefaction, J. Anal. Appl. Pyrolysis. 86 (2009) 331–337, https://doi.org/10.1016/j.jaap.2009.08.006.

[47] B.K. Via, S. Adhikari, S. Taylor, Modeling for proximate analysis and heating value of torrefied biomass with vibration spectroscopy, Bioresour. Technol. 133 (2013) 1–8, https://doi.org/10.1016/j.biortech.2013.01.108.

[48] K. Tasaki, Chemical-free recovery of protein from cow manure digestate solid and antioxidant activity of recovered protein, Environ. Challenges. 4 (2021), 100132, https://doi.org/10.1016/j.envc.2021.100132.

[49] M. Fuentes, R. Baigorri, G. González-Gaitano, J.M. García-Mina, The complementary use of 1H NMR, 13C NMR, FTIR and size exclusion chromatography to investigate the principal structural changes associated with composting of organic materials with diverse origin, Org. Geochem. 38 (2007) 2012–2023, https://doi.org/10.1016/j.orggeochem.2007.08.007.

[50] T. Carballo, A.E. Ma, V. Gil, A.E. Xiomar, G. Ae, F. González, A. Ae, A. Morán, Characterization of different compost extracts using Fourier-transform infrared spectroscopy (FTIR) and thermal analysis, (2008). doi:10.1007/s10532-008-9184-4.

[51] M.B. Hay, S.C.B. Myneni, Structural environments of carboxyl groups in natural organic molecules from terrestrial systems. Part 1: Infrared spectroscopy, Geochim.

Cosmochim. Acta. 71 (2007) 3518–3532, https://doi.org/10.1016/j.gca.2007.03.038.
[52] W.H. Chen, J. Peng, X.T. Bi, A state-of-the-art review of biomass torrefaction, densification and applications, Renew. Sustain. Energy Rev. 44 (2015) 847–866, https://doi.org/10.1016/j.rser.2014.12.039.
[53] J. Scheirs, G. Camino, W. Tumiatti, Overview of water evolution during the thermal degradation of cellulose, Eur. Polym. J. 37 (2001) 933–942, https://doi.org/10.1016/S0014-3057(00)00211-1.
[54] M. González Martínez, A. Anca Couce, C. Dupont, D. da Silva Perez, S. Thiéry, X. mi Meyer, C. Gourdon, Torrefaction of cellulose, hemicelluloses and lignin extracted from woody and agricultural biomass in TGA-GC/MS: Linking production profiles of volatile species to biomass type and macromolecular composition, Ind. Crops Prod. 176 (2022) 114350. doi: 10.1016/j.indcrop.2021.114350.
[55] B. Cämmerer, W. Jalyschko, L.W. Kroh, Intact carbohydrate structures as part of the melanoidin skeleton, J. Agric. Food Chem. 50 (2002) 2083–2087, https://doi.org/10.1021/jf011106w.
[56] X. Guo, J. Huang, Y. Lu, G. Shan, Q. Li, The influence of flue gas desulphurization gypsum additive on characteristics and evolution of humic substance during co-composting of dairy manure and sugarcane pressmud, Bioresour. Technol. 219 (2016) 169–174, https://doi.org/10.1016/j.biortech.2016.07.125.
[57] A. Espina, S. Sanchez-Cortes, Z. Jurašeková, Vibrational Study (Raman, SERS, and IR) of Plant Gallnut Polyphenols Related to the Fabrication of Iron Gall Inks, Molecules. 27 (2022) 279, https://doi.org/10.3390/molecules27010279.
[58] M. Fuentes, R. Baigorri, J.M. Garcia-Mina, Maturation in composting process, an incipient humification-like step as multivariate statistical analysis of spectroscopic data shows, Environ. Res. 189 (2020), 109981, https://doi.org/10.1016/j.envres.2020.109981.
[59] J.A. Rufián-Henares, S.P. De La Cueva, Antimicrobial activity of coffee melanoidins - A study of their metal-chelating properties, J. Agric. Food Chem. 57 (2009) 432–438, https://doi.org/10.1021/jf8027842.
[60] M.C. Millan-Linares, S. Montserrat-de la Paz, M.E. Martin, Pectins and olive pectins: From biotechnology to human health, Biology (Basel). 10 (2021) 860, https://doi.org/10.3390/biology10090860.